Quantifying Erosion and Pollution from Rainfall Runoff on Urbanized Beaches - Galveston Island Study

Final Report

Prepared by

Youn-Kyung Song and Jens Figlus
Department of Ocean Engineering, Texas A&M University / TEES

Kimberly Danesi and Sheryl Rozier
Park Board of Trustees of the City of Galveston, Galveston, Texas

Prepared for

the **Texas General Land Office**

This report was funded in part by a Texas Coastal Management Program grant approved by the Texas Land Commissioner, providing financial assistance under the Coastal Zone Management Act of 1972, as amended, awarded by the National Oceanic and Atmospheric Administration (NOAA), Office for Coastal Management, pursuant to NOAA Award No. NA20NOS4190184. The views expressed herein are those of the author(s) and do not necessarily reflect the views of NOAA, the U.S. Department of Commerce, or any of their subagencies. Additional support was provided by the Park Board of Trustees of the City of Galveston and Texas A&M University.

June 2023

Executive Summary

An investigation into the peak discharge rates and associated stream power of rainwater runoff capable of causing chronic flooding, erosion, and contamination problems on Galveston Island urban beaches was carried out. Galveston Island is a barrier island located on the upper Texas Gulf coast and features an anthropogenically altered shoreline that includes beach nourishments, groins, and a seawall fronting the beach. While most of the island's surface water drains to the bay side, a portion of rainfall runoff drains onto the low-lying, low-gradient (1~2°) coastal beaches. Urban runoff streams can create deep scour channels on the low-permeability beach surface that can transport runoff water eroded soil material and pollutants into the nearshore area of the Gulf of Mexico.

The present study investigated the urban coastal runoff characteristics based on the hydrology assessment of the drainage conditions of the low-lying sand beach of Galveston Island. The potential stream power of the rainfall runoff was quantified and related to local beach surface erosion and downstream beach water quality. Field geomorphology measurements were collected to support this quantification effort. Three major aspects are emphasized throughout the study: 1) quantifying the potential rainfall-runoff relationship with beach drainage volumes, 2) developing a runoff sediment transport formula to estimate the rate of surface soil displacement induced by the beach runoff, and 3) investigating the relationship between rainfall runoff and bacteria level changes in nearshore waters.

A desktop hydrologic analysis was performed to evaluate beach runoff catchment characteristics and to quantify the potential stream power of the peak runoff discharge at two urban Galveston beach sites. A series of low-altitude photographic field survey data collected after various rain events was used to develop a site-specific geomorphic law describing the potential runoff beach erosion as a function of runoff discharge rate and surface gradient over the major beach runoff catchment. The study further investigated the statistical relationship between rainfall event and change in the bacteria level in coastal waters based on the record of Enterococcus concentration reported by the Texas Beach Watch Program (Texas General Land Office, 2015). Finally, recommendations for future coastal storm water studies are made.

Table of Contents

List of Figures

List of Tables

1 Introduction

The City of Galveston is the United States' largest island community established on a barrier island, bounded by the Gulf of Mexico in the south and Galveston Bay in the north. The regional climate creates periodic tropical storms or hurricanes and rainfall events that can become intense locally creating detrimental environments for flood-prone downstream properties. The existing sewer and drainage systems for Galveston Island were primarily designed to drain to the north into Galveston Bay, although a considerable volume of storm water from surface runoff and local outfall drainage systems flows south across the low-lying coastal beaches to discharge into the Gulf of Mexico (City of Galveston, 2003).

Galveston Island beaches are formed in the low-lying coastal plain sloping toward the Gulf of Mexico with a low gradient (1~2°). Vegetation is sparse and fine sand materials create a relatively impermeable surface (Galloway et al., 2003; Morton, 1983). Rainfall runoff conveyed over densely populated overland impervious surfaces can rapidly converge and drain onto the beach as is the case along the entire Galveston seawall where a four-lane road, parking strip, and adjacent land plots drain onto the beach. The concentrated runoff flows can cause sediment surface washouts and deep incision which can pose a hazard to breach users and expose infrastructure foundations (e.g., seawall and pier pilings). In addition, these urban runoff streams directly carry pollutants from developed areas onto the beach and into the nearshore zone leading to potential health risks and beach closures.

To help develop effective engineering solutions to mitigate the rainwater-induced beach flooding and erosion, a simple sediment transport model was developed that can relate the small-scale landform change on the beach downstream to flow routines and discharge rates of the overland runoff streams. Conventionally, the geomorphological changes associated with rainwater flows have been described by a simple transport law evaluating the balance between the stream power of the concentrated channel flows and the resistance of the surface sediment materials (Dietrich et al., 2003; Kirkby, 1971). With advancement in remote sensing and digital elevation model (DEM) technologies, desk base quantification of the runoff physics parameters (slope, paths, and drainage area) has become assessable at a finer scale (i.e., less than 3 meters of spatial resolution). By integrating the high-resolution DEMs with the overland land use, surface sediment characteristics, and regional precipitation databases within a geographical information system (GIS), estimates of rainfall-runoff relationships and potential stream power of the runoff discharge flow can be made at the local catchment scale.

However, the coastal morphologic response to the overland runoff discharge is a complicated process to predict since it involves the complex interplay between stochastic rainfall and discharge events, heterogeneity in sediment material and land surface properties, and spatial variability of the morphological measurements. (Bizzi and Lerner, 2015; Dietrich et al., 2003; Phillips and Slattery, 2007). In order to describe the linkage between runoff flow hydrologic power and

geomorphic erosion (i.e., soil detachment) and sediment transport process via a single transport law, field measurements and parameterization that can validate the existing models for surface erosion or sediment transport are required at a relevant catchment scale (Dietrich et al., 2003; Gartner, 2016; Nachtergaele et al., 2002).

The urban runoff streams directly carry pollutants from developed areas to the shoreline and create deep scour channels on the beach (O'Neill, 1985; Otvos, 1999). The incision channel might function as an efficient transport way conveying the runoff water and eroded soil materials towards the catchment downstream (Nachtergaele et al., 2002; Steegen et al., 2000). The Texas General Land Office (TGLO) manages the Texas Beach Watch program (TBWP) that monitors the Enterococcus bacteria levels on Texas' recreational beaches and provides the public with information about water quality. Enterococci is one of the common fecal coliform bacteria that has been found in the intestines of warm-blooded animals and has the ability to survive in saltwater. Therefore, Enterococci level is often used to monitor contamination of coastal waters by human and/or animal fecal material washed off from land. Analyzing the variability of the Enterococci level at the major outfall points of coastal runoff drainage can inform the environmental impacts of rainwater surface discharge on the receiving waterbody.

The present study aims at investigating the urban coast runoff characteristics based on the hydrology assessment of the drainage conditions of the low-lying sand beach in Galveston Island. It further aims at quantifying the potential stream power of the rainfall runoff and relating them to the local beach surface erosion and downstream beach water quality by supplementing it with field geomorphology measurements. Three major aspects are emphasized throughout the current study: 1) quantifying the potential rainfall-runoff relationship in the beach drainage, 2) developing a runoff sediment transport formula to estimate the rate of surface soil displacement induced by the beach runoff, and 3) investigating the relationship between rainfall runoff and bacteria level changes in the coastal receiving water.

The first part of this report describes the assessments of the rainfall-runoff relationships for Galveston Island beach drainages. First, two target beach runoff sites are introduced to characterize the typical topographic settings and drainage conditions of Galveston Island's urban beaches. The primary runoff flooding and erosion problems were described for the respective beach sites. Next, the runoff catchment delineation is carried out by analyzing the high-resolution regional surface elevation models and theoretical peak runoff rates are calculated according to the Rational Method accounting for the site overland surface soil and land use conditions. The runoff discharge quantities were further assessed to calculate the potential runoff stream power as a hydrologic capacity to induce beach geomorphic change or surface sediment displacement.

The second part of this report describes the field study conducted on the respective target beach sites to measure the typical pattern of runoff surface erosion by means of low-altitude aerial photographic surveys utilizing a UAS (unmanned aerial system; i.e., drone). The geomorphic

properties of the observed eroded features are provided by measuring the changes in length, width, and slope of the target beach surface features. These field geomorphic parameters are then used to formulate the geomorphic relationship between the local runoff stream power and downstream beach surface erosion. In the last part of this report, the potential correlation between rainfall, runoff and bacterial (Enterococcus) level change are investigated based on the published TBWP database reported from the monitoring station closest to the respective target beach sites. The report concludes with summary and a brief discussion of future coastal storm water study needs.

2 Background

2.1 Runoff Drainage Conditions and Issues on Galveston Island Beaches

Galveston Island (Figure 1) discharges excess overland rainwater runoff flows into the Gulf of Mexico after crossing low-lying beach catchment areas. The east Galveston beaches feature a low-gradient, fine sand surface whereas the central beaches are directly connected to the paved surface of urban overland and the Galveston Seawall. This section provides an overview of the existing drainage conditions and primary rainfall runoff issues identified for the eastern and central Galveston Island beach catchments.

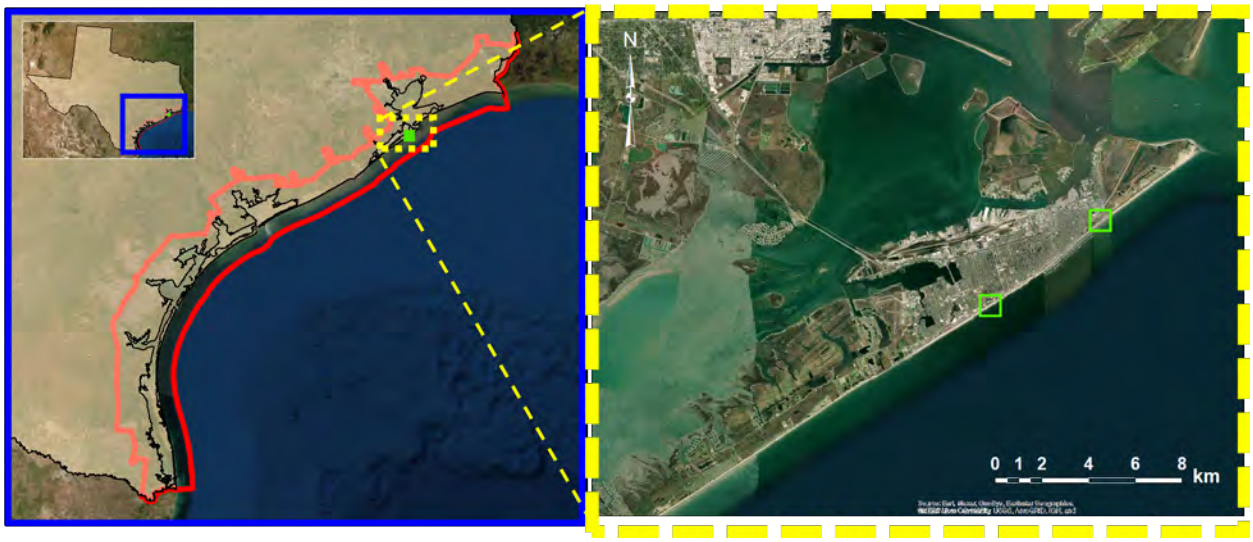

Figure 1. Satellite images showing Galveston Island, Texas. The close-up image on the right shows the locations of the two beach runoff study sites (green solid frames).

2.1.1 Eastern Beaches

The beaches on the eastern part of Galveston Island, such as Stewart Beach, have experienced frequent beach closures due to flooding in parking areas and have developed significant beach scour channels after rainfall events (Figure 2). They are fronted by mostly unpaved parking lots and/or sparsely vegetated sand dunes. The fine soils composing the beach surface tend to exhibit near impervious drainage characteristics that can hinder infiltration of the surface water into the

sediment (National Research Council, 2008). The wet sand present on the beach surface after rainfall can exacerbate unwanted pooling and can make the area vulnerable to erosion by rainfall runoff and tidal water intrusion.

2.1.2 Central Beaches

The central Galveston Island region is comprised of nourished beaches fronting the Galveston Seawall. The regional sewer system was designed to drain stormwater to the north toward Galveston Bay. However, some excess surface water is conveyed to the south by crossing the residential and commercial areas consisting of paved roads, parking lots, and industrial open lands. The nourished beach formed in front of the Galveston Seawall serves as a receiving basin for the urban runoff flow. Overland flows can quickly run down the bluff edge of the seawall at speeds exceeding 1 m/s (3 ft/s). Such a rapid discharge can create deep beach scours in some areas at the base of the seawall with scour depths exceeding 1.2 m (4 ft) below the regular sand surface elevation (Kelly DeSchaun, email correspondence with Helen S. Young, April 17, 2013). The beach scours (Figure 3) can dislodge a sizeable volume of sediment from the beach surface and provide direct discharge routes for the urban runoff waters to the ocean.

Figure 2. Photos of rainwater ponding (top) and a runoff scour channel (bottom) meandering toward the open coast on the Eastern Beach (EB) site after rainfall events. Photos by Youn-Kyung Song, date: 02-09-2018 (top) and 03-22-2021 (bottom).

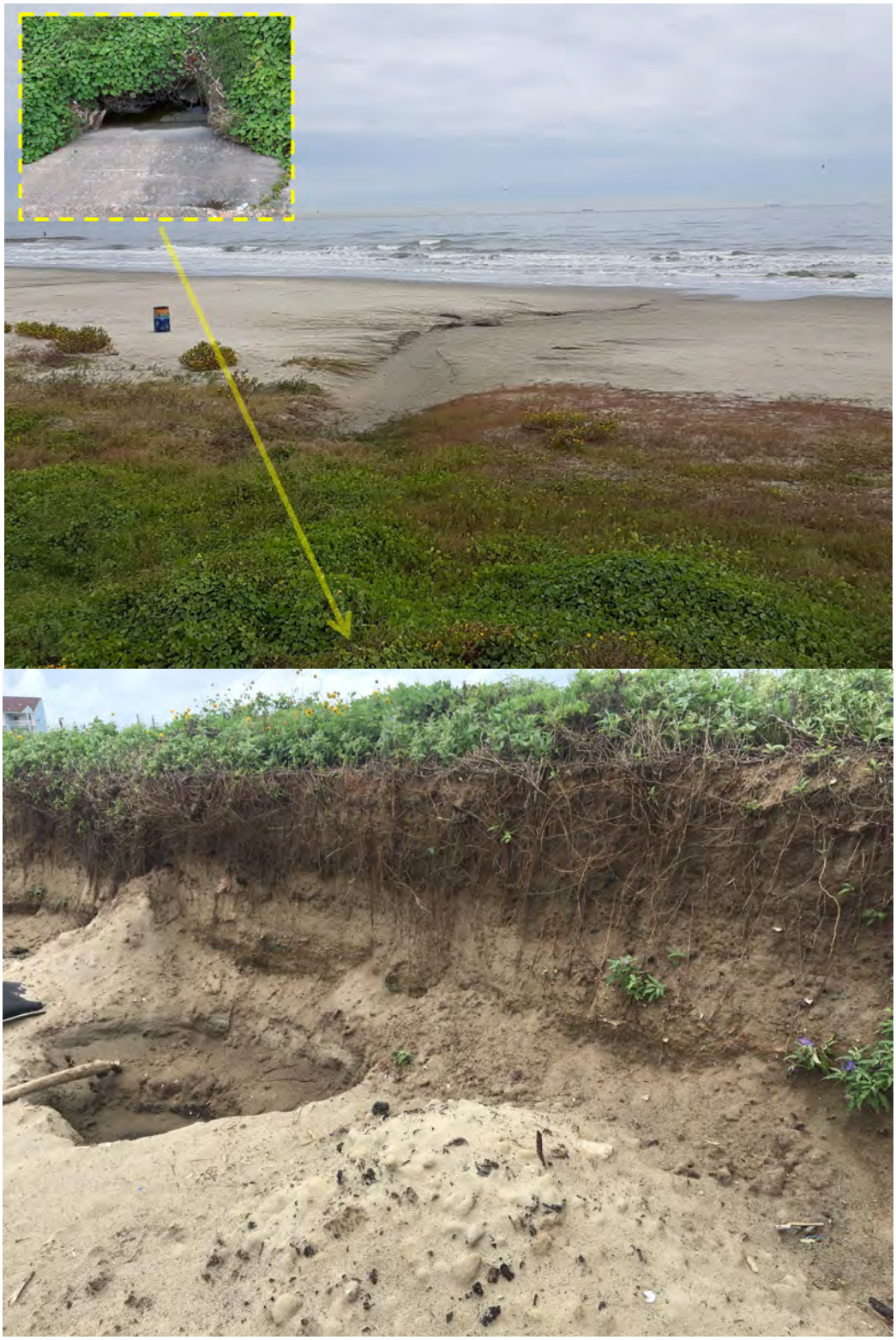

Figure 3. Photos of a runoff scour channel at the seaside toe of the Galveston Seawall (top) and a runoff scour hole at the base of the dune scarp at the Central Beach site. Photos by Youn-Kyung Song (top, date: 03-22/2021) and Jacob Garret (bottom, date: 07-08-2021).

2.2 Study Sites

Based on the major rainwater runoff issues and relevant beach drainage conditions identified in the eastern and central Galveston Island beaches, two beach runoff study sites were selected for detailed hydrologic assessments. Stewart Beach and the beach in front of the seawall across 53rd Street are the selected target sites representative of the drainage conditions at eastern and central beaches, respectively. Figure 4 shows the longshore extent of the target site in the eastern beach (EB) and central beach (CB) of Galveston Island, TX.

Table 1 provides the bounding coordinates (Easting and Northing) of each area of investigation in the UTM coordinate system (Zone 15N). Close-up views of the respective target sites are provided in Figure 5 and Figure 6.

Figure 4. Google Earth™ satellite image of Galveston Island with blue strips ( ) indicating location and alongshore extent of two target runoff study sites located on the eastern and central beach areas of Galveston.

Table 1. East and west boundary locations of the study sites.

Beach Site	Boundary	Easting (m)	Northing (m)
Eastern Beach (Stewart Beach)	East	328690.64	3243379.83
	West	327656.65	3242435.42
Central Beach (53rd & Seawall Blvd)	East	326039.12	3241245.32
	West	324623.07	3240222.97

Figure 5. Zoomed in satellite image of Stewart Beach (Eastern Beach study site). The corner brackets (⌜⌝) mark the north-east and south-west boundaries (Table 1) of the target unmanned aerial vehicle (UAV) survey area. Sediment samples were collected at the location marked by a cross (+).

Figure 6. Zoomed in satellite image of the Central Beach study site located south of Seawall Boulevard between two groins in the vicinity of 53rd Street. The corner brackets (⌞⌝) mark the north-east and south-west boundaries (Table 1) of the UAV survey area. Sediment samples were collected at the location marked by a cross (+).

Surface sediment samples were collected from each beach site during field reconnaissance and a sieve analysis was carried out to evaluate grain compositions in the runoff beach catchment areas. The size distributions of the surface sediments (Appendix – A1) indicate average grain sizes of 0.15 mm and 0.16 mm for the EB and CB sites, respectively, and that more than 50 % of the sediments are finer than 0.15 mm in diameter.

3 Methodology

3.1 Rainwater Runoff Quantification

Hydrologic analysis was performed using the Rational Method (RM) expressed as:

$$Q_{\mathrm{p}} = \frac{CIA}{\mathrm{Z}} \qquad (1)$$

Here, Q_{p} is the peak runoff discharge rate (ft^3/s or m^3/s), I is the average rainfall intensity (in/hr or mm/hr), A is the runoff catchment area (acre or hectare), and Z is the conversion factor, 1 for English, 360 for metric units. The non-dimensional runoff coefficient C is determined based on land use, cover imperviousness, and hydrologic soil type. The RM assumes that the rainfall intensity is uniform throughout the duration of the peak-producing rainfall and that the rainfall is distributed uniformly over the contributing drainage area. The RM further assumes that any available surface water storage has been filled to maximum capacity.

The catchment analysis was conducted using the spatial analysis tools within ArcGIS (ArcMap 10.4). First, the connectivity and hierarchy (i.e., stream order) of the potential runoff streams were evaluated in order to calculate the catchment area A, maximum flow length L, and average slope S. The 1/9 arc-second resolution (approx. 3 meters), seamless national elevation database (NED) DEMs (USGS, 2017) were used as input rasters.

The runoff coefficient C accounts for the surface characteristics such as land gradient, soil type, vegetation condition, and land use. C approaches unity with an increase in surface slope or surface imperviousness and reduces in value as infiltration capacity increases. Recommended values for C are C = 0.70 – 0.90 for low to high development areas and open spaces, C = 0.60 for barren land, and C = 0.20 – 0.25 for vegetated areas (TxDOT, 2016; USDA-NRCS, 2010; Li and Chibber, 2008; Roussel et al., 2005; WEF and ASCE, 1992; USDA-SCS, 1947). For areas with a mixture of land use, composite runoff coefficients are calculated by weighting the area of respective land use (TxDOT, 2016).

The composite runoff coefficients for C were calculated based on surface soil and overland use conditions of each runoff site. The national hydrologic soil group (HSG) data developed by the U.S. Department of Agriculture-National Resources Conservation Service (USDA-NRCS, 2014; https://websoilsurvey.nrcs.usda.gov/) provides a digital soil map characterizing the spatially varying hydrologic soil conditions. The USDA-NRCS hydrologic soil data assigns surface soils to one of four groups (A, B, C, or D) or dual soil groups (e.g., A/D) where the soil group ‘A’ represents the most pervious condition and ‘D’ the most impervious condition. In the case of the dual soil group, the first letter applies to the drained condition and the second applies to the undrained condition. According to the HSG classification, the condition of the coastal land of Galveston Island is characterized largely as either group D or A/D type soils and undrained soil

conditions can be assumed. Therefore, the hydrologic group D soil type was assumed in the peak runoff rate evaluations for the respective beach sites.

The recommended values of the runoff coefficient C for type "D" hydrologic soils (TxDOT, 2016; WEF and ASCE, 1992) were then assigned to different land use classifications provided in the 2011 National Land Cover Data by the Multi-Resolution Land Characteristics Consortium (MRLC Consortium, 2011; http://www.mrlc.gov/). Once the individual sub-catchment areas were delineated (based on the DEM), the area averaged runoff coefficients were calculated for the EB and CB sites, respectively, to represent the runoff discharge conditions depending on surface soil and land use condition.

The rainfall intensity I was determined according to the power-law model developed based on the probabilistic rainfall intensity-duration-frequency (IDF) relationship (Asquith and Roussel, 2004; Cleveland et al., 2015) as:

$$I = \frac{b}{(t_C + d)^e} \tag{2}$$

The coefficients e, b, and d for I vary depending on the rainfall annual return periods (ARP). Table 2 presents the rainfall IDF coefficients suggested for use in the power-law model evaluating the rainfall intensity for Galveston County, TX, for different Annual Event Probability (AEP) and Annual Return Interval (ARI) values.

Table 2. Rainfall IDF coefficients for Galveston County, TX

AEP (in percent)	ARI (in years)	b	d	e
50 %	2	58.30	11.04	0.7839
20 %	5	70.47	12.60	0.7636
10 %	10	77.97	13.38	0.7496
4 %	25	91.45	14.79	0.7430
2 %	50	99.26	14.85	0.7308
1 %	100	115.89	16.50	0.7295

The time of concentration t_c (in minutes) is determined as a function of L and S, and is the sum of the overland flow time t_{ov} and the channel flow time t_{ch}. For urban runoff catchments, t_c is often estimated by the Kerby-Kirpich method (Roussel et al., 2005). The Kerby-Kirpich method is suitable for watersheds with sizes smaller than 150 square miles (9600 acres), a length of overland flow no longer than 1,200 feet (366 meters), main channel lengths between 1 and 50 miles (1.6 and 80.5 km), and main channel slopes between 0.002 and 0.02 (ft/ft) (Roussel et al., 2005).

The Kerby-Kirpich method estimates the total time of concentration by adding the overland flow time t_{ov} and the channel flow time t_{ch}:

$$t_c = t_{ov} + t_{ch} \quad (2)$$

For small watersheds as in our case here where the overland flow is an important component of overall travel time, the Kerby method can be used (Roussel et al. 2005).

$$t_{ov} = \mathrm{K}(L_{ov} \times N)^{0.467} S^{-0.235} \quad (3)$$

where

t_{ov} = overland flow time of concentration, in minutes

K = unit conversion coefficient, with K = 0.828 for English units and K = 1.44 for SI units

L_{ov} = overland-flow length, in feet or meters as dictated by K

N = dimensionless retardance coefficient

S = dimensionless slope of the terrain conveying the overland flow

The upper limit of L_{ov} is 1200 ft (366 meters). A flow path exceeding this upper limit is converted to a concentrated channel. The dimensionless retardance coefficient N for the overland flow varies from 0.02 to 0.80, depending on land cover characteristics (TxDOT, 2016).

The time component of the concentrated channel flow runoff t_{ch} is estimated as:

$$t_{ch} = K{L_{ch}}^{0.770} S^{-0.385} \quad (4)$$

where

t_{ch} = time of concentration, in minutes

K = unit conversion coefficient, where K = 0.0078 for English units and K = 0.0195 for SI units

L_{ch} = channel flow length, in feet or meters as dictated by K

S = dimensionless main channel slope

An adjustment to the slope value used for the calculation of t_c is suggested for watersheds with low topographic slope (flat terrain) with average slopes less than 0.002 ft/ft (0.2%). This helps avoid unreasonably large values of t_c. The adjusted slope should be S_{low} = S + 0.0005 (Cleveland et al. 2012). In this study, the adjusted slope S_{low} is used for areas with slopes equal to or less than 0.002 ft/ft (0.2%).

3.2 Runoff-Sediment Displacement Relationship

The surface erosion can be caused by both sheet wash and concentrated channel flows. In general fluvial physics, surface erosion is assessed mechanically based on a geomorphic transport law linking the rate of surface erosion (soil detachment) q_s with the stream power of the surface flow (Dietrich et al., 2013; Horton, 1945; Howard and Kerby, 1983; Meyer-Peter and Muller, 1948). The stream power Ω is the water's potential energy (PE) that is necessary to maintain and carry the particle in motion over a unit length (Bagnold, 1966). The stream power formula can be expressed using catchment parameters as:

$$\Omega = \frac{\Delta PE}{\Delta t} = mg\frac{\Delta z}{\Delta t} = \rho g Q_p S \tag{3}$$

where m is water mass, g is gravitational acceleration (9.8 m/s^2), t is time, z is elevation, ρ is the density of water (1000 kg/m^3), Q_p is the peak runoff discharge rate (m^3/s), and S is the average slope within the runoff catchment.

The geomorphic transport law relates the surface stream power to the mass rate of soil detachment or sediment transport q_s observed in a specific scale (in time and space). The practical geomorphic transport law can be expressed using the runoff hydrologic parameters as (Dietrich et al., 2003; Meyer-Peter and Muller, 1948):

$$q_s = \frac{\partial Vol}{\partial t} = \frac{\partial d_e}{\partial t} W_e L_e = V_R W_e L_e \tag{4}$$

where $q_s = \partial Vol/\partial t$ is the volume rate of the soil detachment or transport (m^3/s or ft^3/s). The left hand side of (4) equates with the product of the effective depth d_e, width W_e, and length L_e of the eroded surface layer (i.e., $Vol = d_e W_e L_e$) scaled by the runoff period t. The incision rate $\partial d_e/\partial t$ is associated with the characteristic runoff velocity along the eroded channel, V_R (m/s or ft/s).

The link between (3) and (4) is made by relating the potential power of the runoff stream to the rate of effective sediment volume displaced during the runoff erosional process as:

$$q_s = V_R W_e L_e = K_e \left(Q_p S\right)^n \tag{5}$$

The left hand side of (5) can be assessed once the runoff channel morphology is determined from field measurements. The right hand side of (4) can be assessed based on the desktop analysis of the runoff hydrologic parameters (as presented in *Ch.4*). The best fit values for K_e and n reflect the overland use and permeability of the surface soil at the runoff site. Note that the parameter S used in the right hand sided of (5) is the average slope of the initial surface of the runoff catchments, which is assessable prior to runoff erosion from the DEM analysis.

4 Results

4.1 Beach Runoff Stream Network and Catchment Characteristics

The peak runoff rates were evaluated in units of water volume per time (ft^3/s) at selected pour points in the central and eastern beach drainage sites of Galveston Island. The pour point is the most downstream outlet of mainstream flows formed by the highest order connection of overland runoff tributaries discharging into the respective beach catchments. Figure 7 and Figure 8 provide the subcatchment boundaries and synthetic stream network assessed for the respective EB and CB sites. The subcatchment boundaries (orange lines) delineate the areal extent of the individual synthetic runoff stream network (blue lines) discharging at a common pour point.

At the EB site the surface water streams were initiated from the developed overland area beyond Seawall Boulevard. The runoff streams are gathered together on the beach after crossing the low-permeability surfaces of the beachside parking lots, intermittent buildings and driveways, and natural vegetation swales. The flow initially running down the steeper, impervious overland surface may lose its momentum as it reaches the flatter, back beach area. The excess stream power produced by the converging discharge streams can create local scour holes and scour channels that can cut through the beach. The fine-grained sand in combination with the low-gradient surface contributes to reducing the conveyance capacity of the surface water by infiltration and gravity flow leading to the chronic flooding often observed on the back beach.

At the CB site the surface streams originate mostly from the paved surface of Seawall Blvd. However, where adjacent beach resorts or businesses have a parking lot with a large impervious footprint, the runoff streams develop from further upland. The resulting runoff network is formed by low-order streams (i.e., 1^{st} or 2^{nd} order). The surface discharge streams run down to the beach rather abruptly without converging along the seaside surface of the seawall structure. The associated runoff travel times and distances are small. In some catchments, t_c is less than 5 minutes. The local peak runoff rates are also predicted to be relatively low. Therefore, the primary runoff issues of beach scour holes at the seawall base and channel cuts identified in the central beach area can be attributed to the short travel path with corresponding rapid runoff response (small L and t_c) and the contrasting high rundown speed.

Figure 7. Runoff catchments and surface stream network calculated for the Eastern Beach site (Stewart Beach).

The primary runoff characteristics of the EB and CB sites are summarized in Table 3 in terms of the runoff input parameters of surface slope S, longest runoff flow pathway L, areal extent A, and time of runoff flood concentration, t_c, for each site. The listed properties were calculated based on the largest subcatchment condition where the predicted runoff flow drained with the highest order of stream link at the pour point (■ in Figure 7 and Figure 8). The locations of the major pour points at the EB and CB sites are provided in UTM coordinates (Zone 15N) in meters.

Figure 8. Runoff catchments and surface stream network calculated for the CB site (53rd Street Beach).

Table 3. Beach runoff catchment parameters and locations of pour points located at the eastern site (EB: Stewart Beach) and central site (CB: 53rd St)

SITE	Easting	Northing	Area		C	Mean Slope	Max. Flow Length		t_c		
									t_{ov}	t_{ch}	$t_{ov} + t_{ch}$
	(UTM, m)	(UTM, m)	(m^2)	(acres)		(%)	(m)	(ft)	(min)	(min)	(min)
EB	328127	3243061	100993	25.0	0.724	1.5	492	1613	19	4	23
CB	323411	3239477	2038	0.5	0.857	4.8	143	470	6	0	6

4.2 Peak Runoff Rate Q_p

Once rainfall duration or t_c is assessed using the Rational Method, the rainfall intensity I can be determined for various recurrence frequencies or AEP according to (2). Table 4 provides the

general values of *I* predicted for rainfall event return intervals of two (2), five (5), ten (10), twenty-five (25), and one hundred (100) years.

Table 4. Rainfall intensities calculated with the power-law model for Galveston County, TX

	I (in./hr)					
	2-year	5-year	10-year	25-year	50-year	100-year
EB	3.6	4.6	5.2	6.1	6.9	7.9
CB	6.3	7.6	8.5	9.6	10.8	12.0

The beach runoff parameters presented in Table 3 and predicted rainfall intensities in Table 4 are combined to calculate the potential peak runoff rates at the respective pour points according to the Rational Method. The peak runoff rates predicted for the given return intervals between two and one hundred years are provided in Table 5.

Table 5. Potential peak runoff rates calculated by the Rational Method for varying rainfall intensities.

	Q = CIA (cfs)					
	2-year	5-year	10-year	25-year	50-year	100-year
EB	65.8	82.7	94.6	110.5	125.2	142.5
CB	2.7	3.3	3.7	4.1	4.7	5.2

The greater catchment area associated with the high-order stream network predicted at the EB site resulted in substantially higher runoff rates compared to the peak runoff predicted at the major pour points at the CB site. The complicated stream pathway network that forms on the mildly sloped beach surface makes the EB site vulnerable to flooding. On the other hand, the beaches in front of the seawall at the CB site receive the direct discharge from low-order overland runoff streams originating from relatively small areas no greater than 1 acre. The overland flows run down rapidly across the impervious surface of the seawall to cause an abrupt outfall impact at the toe of the structure producing scour holes on the beach surface at the seawall base and deep channel cuts expanding toward the shoreline.

4.3 Measured Runoff-Induced Beach Surface Erosion

The impact of runoff discharge on beach surface erosion was investigated by means of low-altitude photographic surveys conducted at both study sites after selected rain events between September 2021 and February 2022. Multiple, overlapping aerial images were collected using a UAV (DJI Phantom3) outfitted with a high-resolution RGB camera and GPS capability. The images were post-processed and fitted together using structure from motion (SfM) techniques and algorithms. SfM approaches trace the position of the camera and scene geometry from image to image and conduct automatic identification of matching features in order to estimate object coordinates in 3-

D space. The resulting 3-D point clouds are aligned to an absolute (i.e., real-world) coordinate system based on a number of ground-control points (GCPs) with surveyed coordinates. The GCP coordinates were obtained via a separate ground survey using RTK GNSS (Real-Time Kinematic Global Navigation Satellite System) surveying equipment.

The field survey focused on capturing the surface geomorphic change near major runoff pour points identified at the EB and CB sites (in Figure 7 and Figure 8).

The geo-rectified image mosaic and DEM products presented in Figure 9 and Figure 10 show the beach surface morphology and elevation contours measured after rain events occurred. The UAV survey product for the EB site exhibits a conspicuous runoff pathway sited downstream of the major catchment shown in Figure 7. The runoff channel formed initially at the narrow opening between existing foredunes and stretched out shoreward. As erosion progressed as far down as the high tide water level, scarping and slumping of the channel edge occurred on both sides. This process expanded the width of the runoff erosion channel as flows also started to interact with the swash zone on the beach.

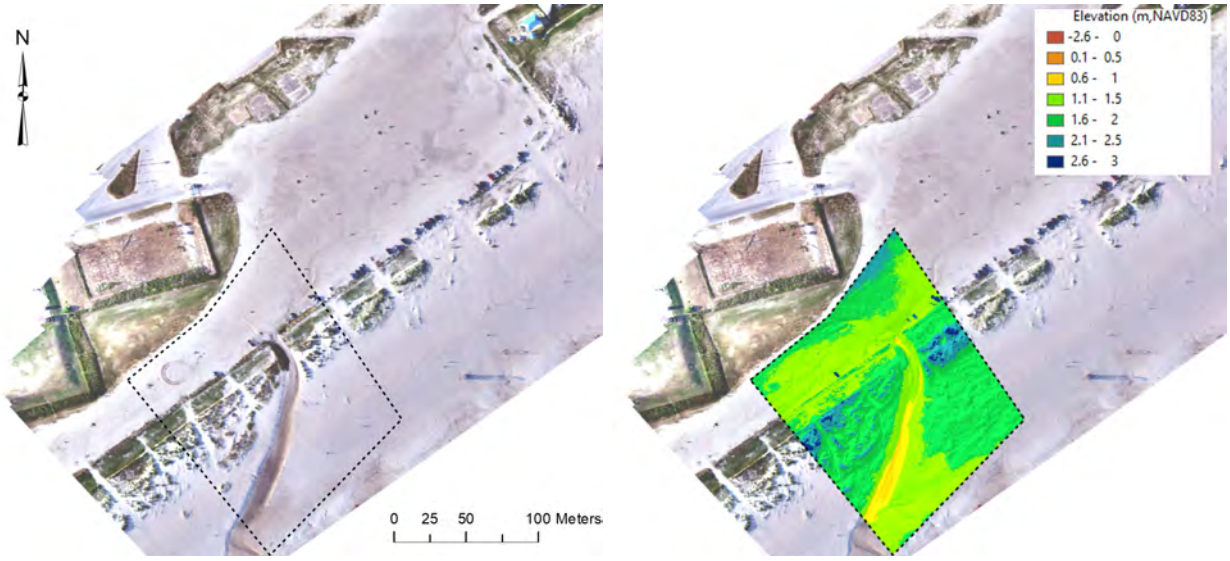

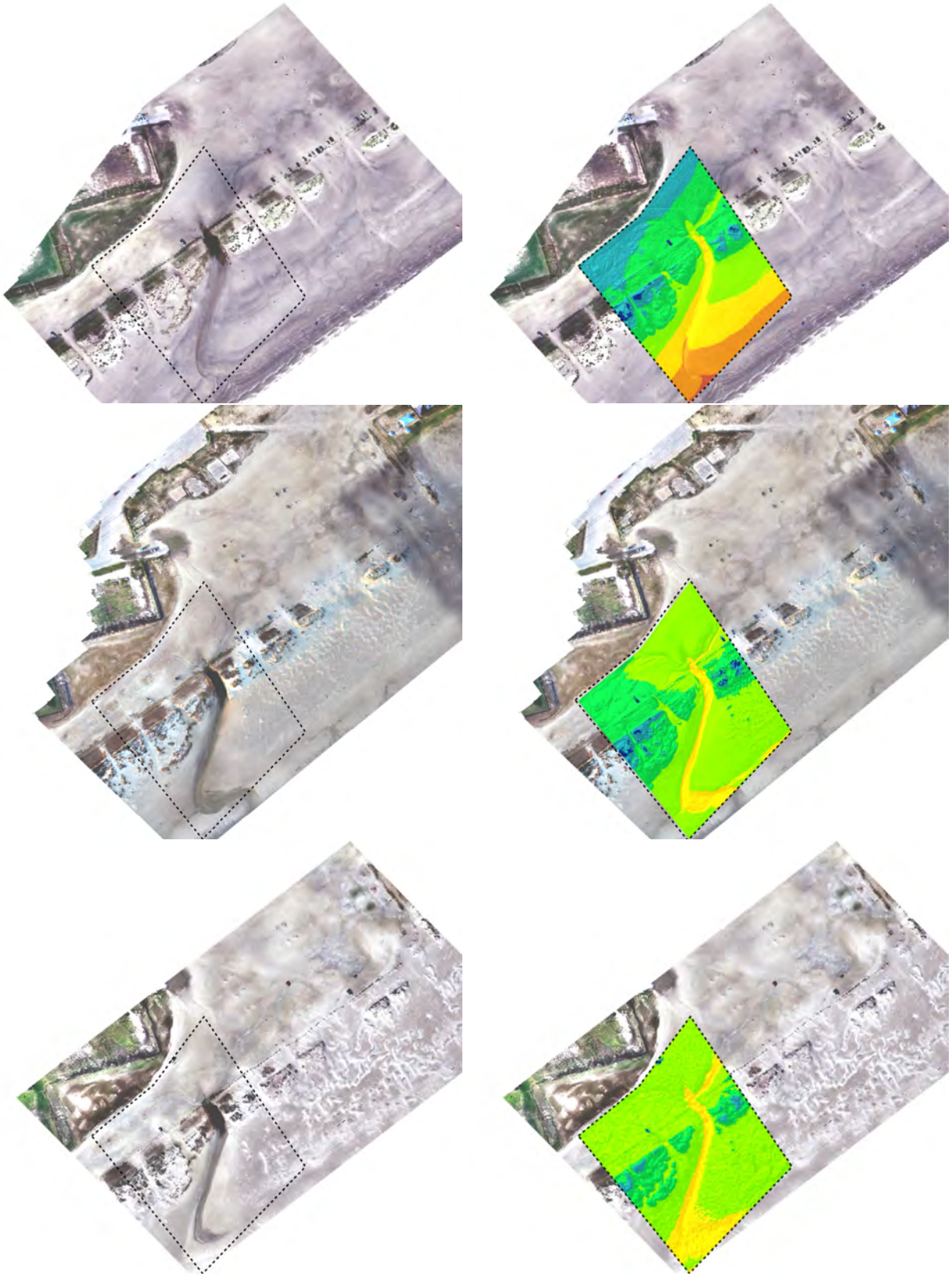

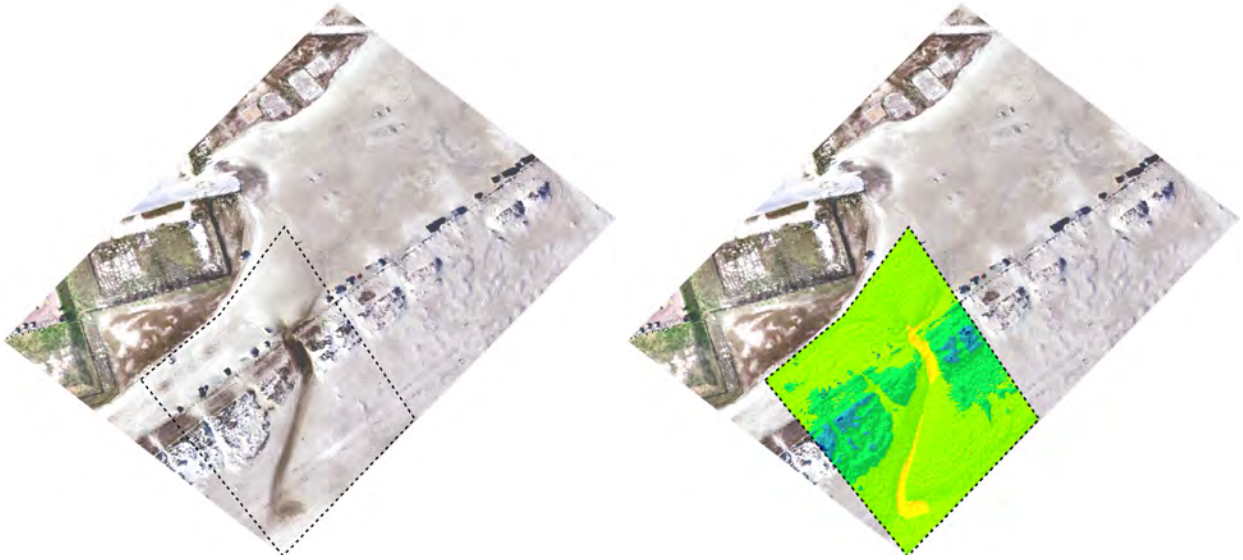

Figure 9. Orthophoto mosaic and DEMs displaying eroded beach surface features and elevation contours for the Eastern Beach site. The georeferenced orthophoto aerial images (left) overlain by the surface DEMs (right) were collected via field UAV surveys on 9/8/2021, 9/20/2021, 12/1/2021, 1/22/2022, and 2/11/2022, respectively (from top to bottom).

In contrast, the beach surface at the CB exhibited the typical erosion pattern caused by rapid urban runoff. The runoff discharge from the connected impervious overland beyond Seawall Blvd. runs down abruptly as low-order streams (i.e., 1st or 2nd order streams) creating most of the erosive impact on the beach surface at the base of the seawall structure. However, the impact from the rainfall experienced during the field measurement period seemed to be damped by the vegetation in front of the seawall leading to relatively minor beach scour holes. After more severe rainfall events, runoff scour holes may extend much farther along the base of the seawall or across the beach fronting it. Such cross-beach runoff channels could provide ephemeral gullies conveying the direct discharge of overland flow offshore and facilitating tidal water intrusion toward the seawall base. For example, the lowered topography in between the seawall base and the start of the beach vegetation observed on 12/3/2021 and 1/22/2022 is connected to the runoff channel cutting through the vegetation patches present upstream of the pour point.

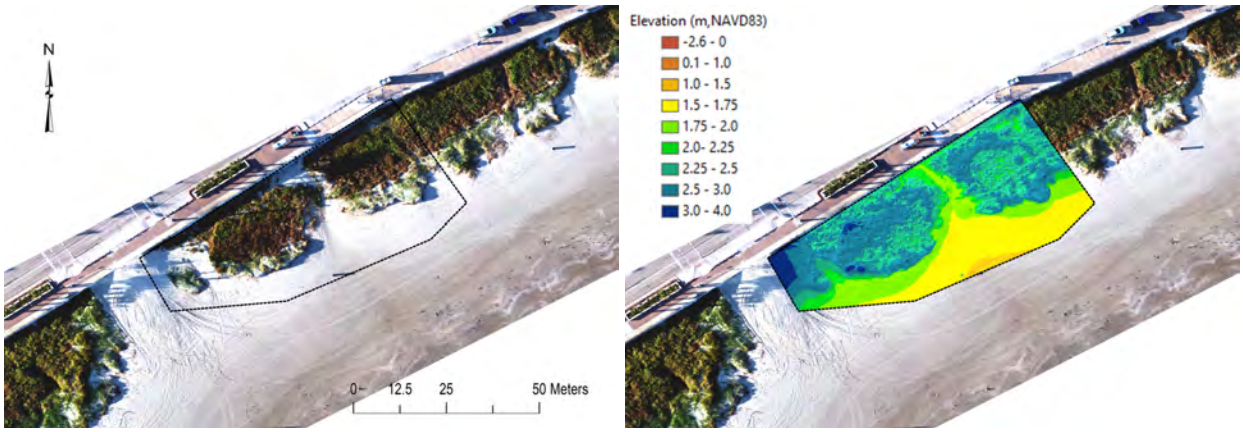

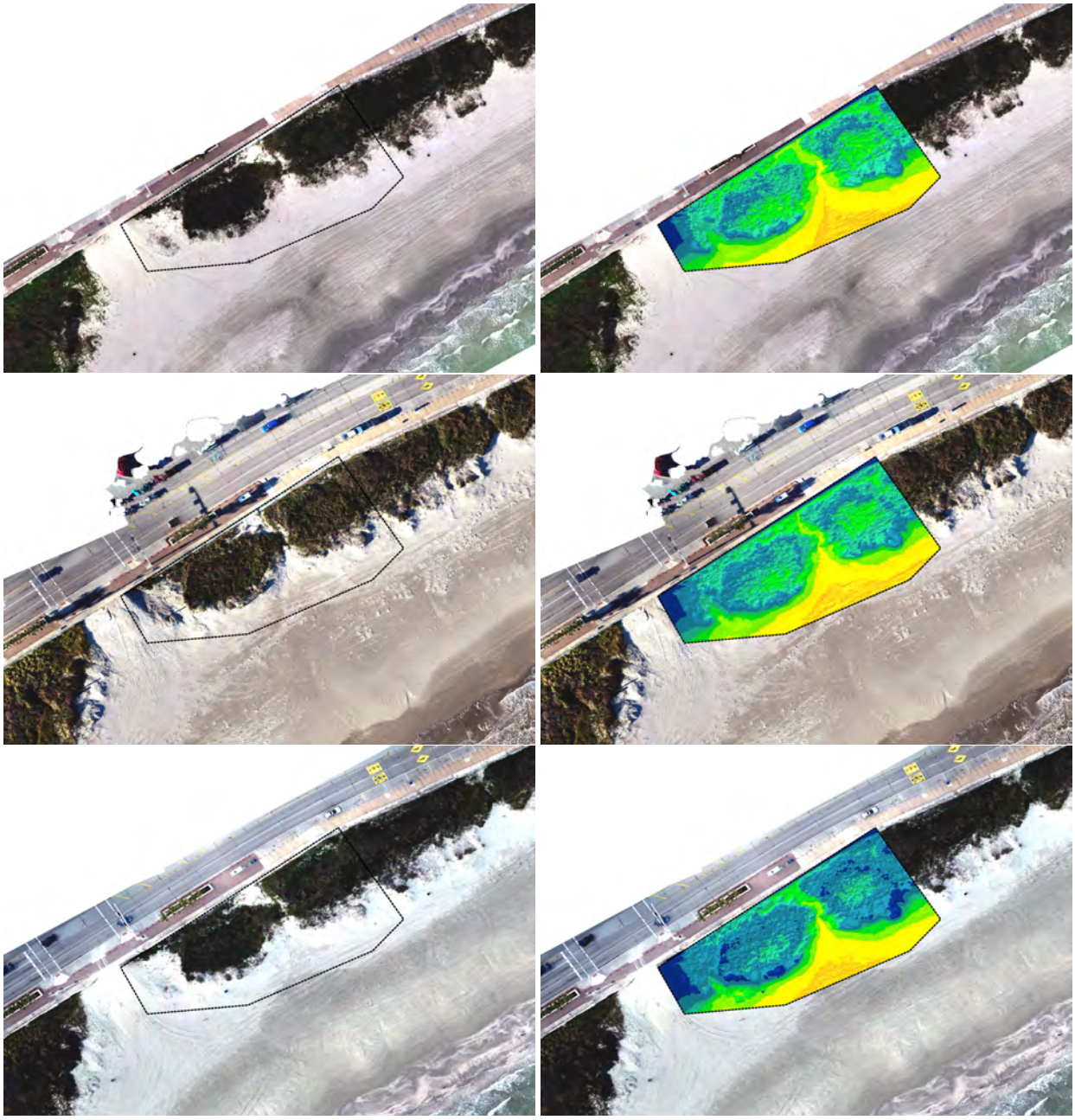

Figure 10. Orthophoto mosaic and DEMs displaying the eroded beach surface feature and elevation contours for the CB site. The georeferenced orthophoto aerial images (left) overlain by the surface DEMs (right) were taken during the field UAV surveys on 9/20/2021, 12/3/2021, 1/22/2022, and 2/11/2022, respectively (from top to bottom).

The beach geomorphic changes were measured in terms of the length (L_e), slope (S_e), and width (W_e) of the eroded feature at the target locations at both field sites. The geomorphic dimensions of the measured beach surface erosion and associated rainfall records are summarized in Table 6 for the EB site and in Table 7 for the CB site.

Table 6. Field geomorphic parameters describing the runoff-erosion relationship calculated for the eastern beach (EB) site.

Site	UVA Survey (m/dd/yyyy)	Rain Event (m/dd/yyyy)	P_{1hr} (in.)	P_{max} (in.)	Q_p (cfs)	Q_{Pmx} (cfs)	V_R (fps)	L_e (ft)	S_e (%)	W_e (ft)
EB	9/8/2021	9/3/2021	0.4	0.8	6.7	13.7	2.0	75	4.2	135
EB	9/20/2021	9/14/2021	0.6	2.3	10.3	39.1	1.5	292	2.2	161
EB	12/1/2021	11/11/2021	0.5	0.5	8.3	7.6	1.4	256	1.7	121
EB	1/22/2022	12/18/2021	0.8	1.0	15.0	18.9	1.3	253	1.5	269
EB	2/11/2022	1/20/2022	0.4	0.7	7.2	13.1	1.4	262	2	131

Table 7. Field geomorphic parameters describing the runoff-erosion relationship calculated for the central beach (CB) site.

Site	UVA Survey (m/dd/yyyy)	Rain Event (m/dd/yyyy)	P_{1hr} (in.)	P_{max} (in.)	Q_p (cfs)	Q_{max} Q_{Pmx}	V_R (fps)	L_e (ft)	S_e (%)	W_e (ft)
CB	9/20/2021	9/14/2021	0.6	2.3	0.2	0.8	1.6	33	2.6	10
CB	12/3/2021	11/11/2021	0.5	0.5	0.2	0.2	2.0	30	4.2	7
CB	1/22/2022	12/18/2021	0.8	1.0	0.4	0.5	2.1	33	4.8	7
CB	2/11/2022	1/20/2022	0.4	0.7	0.2	0.4	2.1	26	4.8	7

At the EB site, L_e was defined as the cross-beach extent of the eroded feature starting from the common pour point to downstream above the depth contour where the meandering channel started to encounter the effect of tidal water flows. At the CB site, L_e was defined as the cross-beach extent of the eroded feature starting from the seawall base to north of the site's high water mark where the surface slope changed significantly. S_e is the mean surface slope over the distance L_e. W_e is the longshore distance between 1.0 m and 1.75 m elevation contours, respectively at EB and CB sites, on either side of the eroded channel. The runoff flow velocity V_R was estimated according to the NRCS (Natural Resources Conservation Service) equation for shallow concentrated flow velocity of nearly bare and untilled overland flow as a function of watercourse slope: $V_R = 9.965(S_R)^{0.5}$ (USDA-NRCS, 2010).

The maximum 1-hour rainfall depth (P_{1hr}) reported during the field measurement period varied between 0.4 and 0.8 in. Additionally, the record of the daily maximum accumulated rainfall depth (P_{max}) is provided which varied from 0.8 to 2.3 in. The potential peak (Q_p) and maximum cumulative rainfall runoff rate (Q_{max}) corresponding to the rainfall depth of P_{1hr} and P_{max}, respectively, were estimated by the Rational Method using (1). The measured geomorphic

properties of the eroded beach surface were compared to the potential power of the runoff stream, both Q_p and $Q_{max,}$ according to (5). Figure 11 and Figure 12 show the runoff-sediment displacement relationship assessed for the EB and CB sites, respectively.

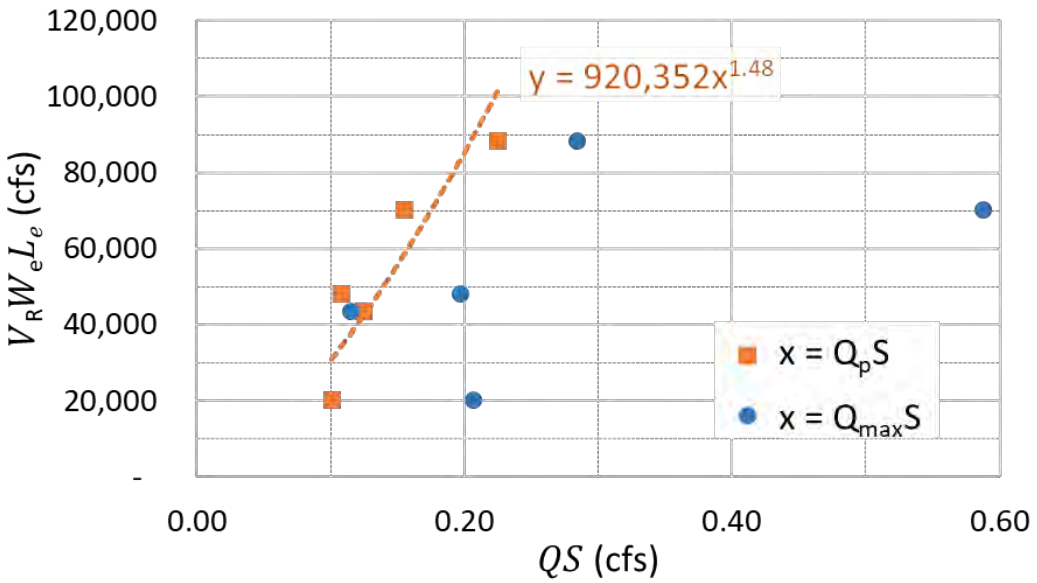

Figure 11. Runoff-sediment displacement relationship evaluated based on the measured beach erosion at the EB site.

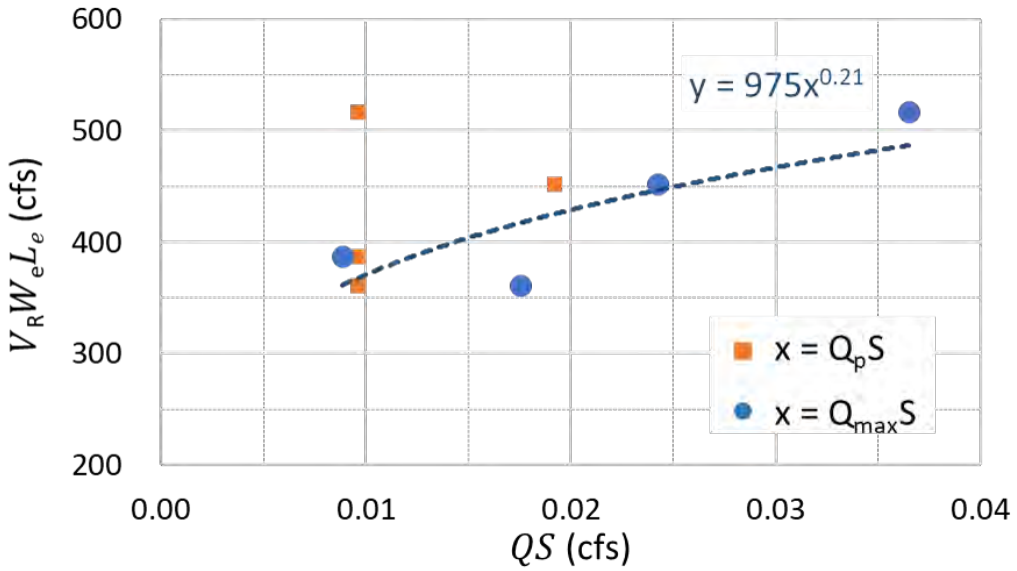

Figure 12. Runoff-sediment displacement relationship evaluated based on the measured beach erosion at the CB site.

The resulting geomorphic relationship indicates that the rate of beach sediment displacement ($V_R L_e W_e$) is most sensitive to the peak runoff rate Q_p at the EB site and most sensitive to the

maximum cumulative rainfall runoff rate Q_{max} at the CB site. The runoff-erosion parameters used in (5) were estimated as K_e = 920,352 and n = 1.48 with the squared correlation coefficient, R^2 = 0.73 for the EB site and K_e = 975 and n = 0.21 with R^2 = 0.62 for the CB site.

4.4 Bacterial Levels in Coastal Waters Downstream of Runoff Catchments

Records of Enterococcus bacteria levels were obtained from nearby Texas beach water monitoring stations (● in Figure 7 and Figure 8). Water samples at the monitoring stations are collected weekly during peak beach season (i.e., March – October) and every two weeks for the rest of the year. The TBWP complies with the action values and standards of the US Environmental Protection Agency (USEPA) Beaches Environmental Assessment and Coastal Health (BEACH) Act of 2000. It requires that the average sample density standard in the marine recreational water is no more than 35 colony forming units per 100 mL (CFU/100 mL) or 35 most probable number per 100 mL of sample volume (MPN/100ml) (USEPA, 2012). The CFUs are determined by directly counting visible colonies of bacteria captured on the membrane filter per volume of the environmental sample. MPN analyses estimate the number of organisms in a sample using statistical probability tables based on the reaction levels in the test tubes containing a special media to which the samples was added at different concentrations. Both units/values are derived from culture-based enumerated method whereas focusing on different attributes of the fecal indicator. EPA recommend that 35 CFU/100 mL or 35 MPN/100 mL is used as the marine water standard value (USEPA, 2012). The measured water quality information is updated on the TBWP website and advisory signs are posted at corresponding beach access points when bacterial levels exceed the set threshold (Texas General Land Office, 2015).

Historical records of rainfall (left vertical axis) and Enterococcus concentrations for the project period ranging from July 2020 to December 2021 are displayed in Figure 13 and Figure 14 for the EB and CB sites, respectively. The bacteria levels (right vertical axis) shown are the daily maxima reported from the respective TBWP station located at the EB (TX451421) and CB (TX486021) sites (https://www.waterqualitydata.us). Correspondingly, the 24-hour maximum rainfall quantities were calculated from historical local precipitation data provided by the Climate Data Online (CDO) system (NOAA: https://www.ncdc.noaa.gov/cdo-web/) at 15-minute intervals.

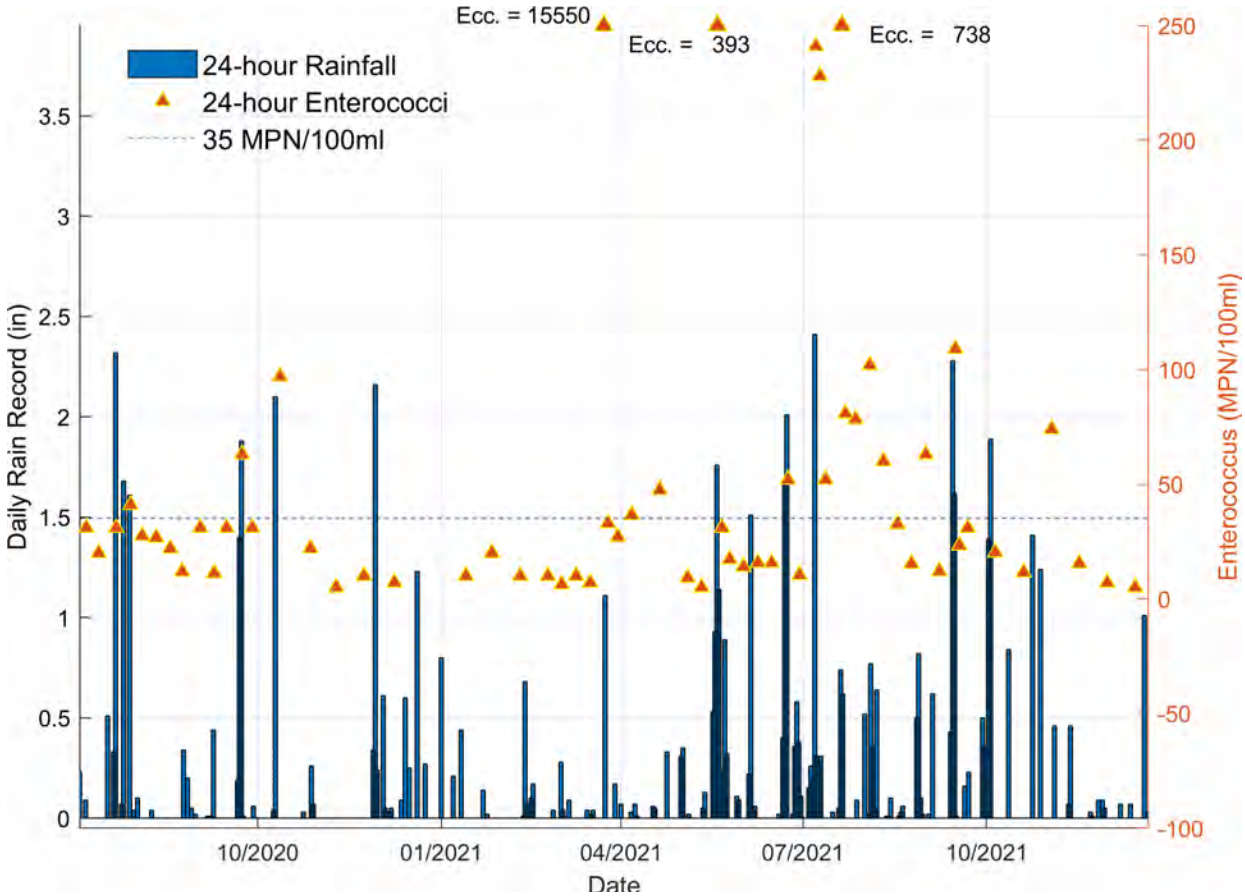

Figure 13. Time series of rainfall record plotted in comparison to the record of Enterococcus concentration for the EB site. 24-hour maximum rainfall quantities (bar chart, left vertical axis) are plotted against the daily maximum Enterococcus bacteria levels (▲, right vertical axis) calculated based on the water quality data obtained from nearby TBWP station TX451421. A number of outstanding records of the Enterococcus concentration are plotted along the upper limit of the right vertical axis with the actual bacterial level noted by the respective numbers adhered.

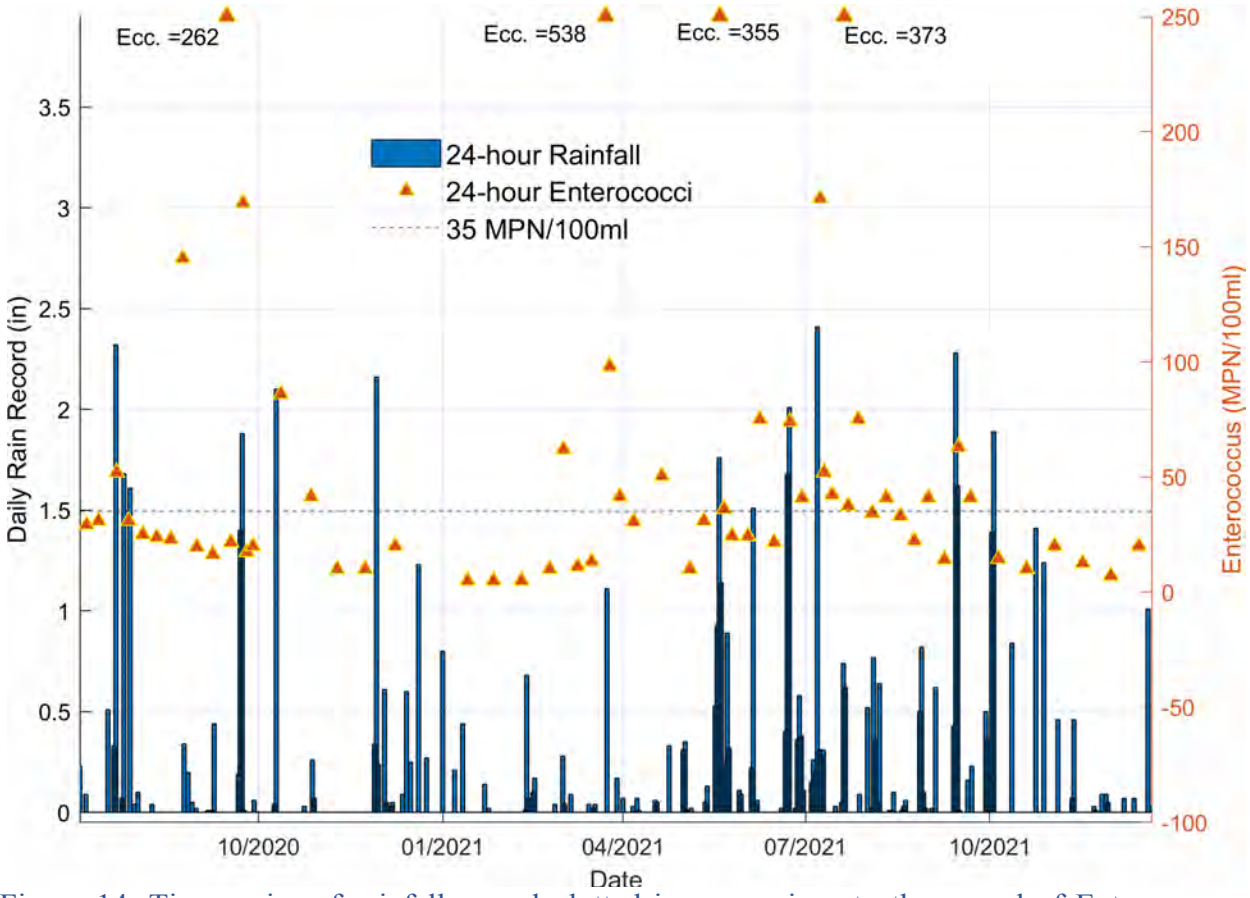

Figure 14. Time series of rainfall record plotted in comparison to the record of Enterococcus concentration for the CB site. 24-hour maximum rainfall quantities (bar chart, left vertical axis) are plotted against the daily maximum Enterococcus bacteria levels (▲, right vertical axis) calculated based on the water quality data obtained from nearby TBWP station TX486021. A number of outstanding records of the Enterococcus concentration are plotted along the upper limit of the right vertical axis with the actual bacterial level noted by the respective numbers adhered.

The average, median, and maximum of the Enterococcus levels recorded after various rain events during the study period are summarized in Table 8 for each beach site. Overall, the Enterococcus concentration rose after rain events of various intensities but values exceeding 35 MPN/100ml were recorded when rainfall persisted for more than one day. The numbers in the last column provide the percentage of exceedances above the USEPA standard value of 35 MPN/100ml using the 550 data points considered in the statistical computations. When bacteria levels exceeded the standard value they were associated with average cumulative rainfall records of 1.1 inches for the EB site and 1.2 inches for the CB site. The increase in bacteria levels became more prominent when heavier precipitation ensued after days with only tenuous rain. During the study period the highest measured bacteria level was 15,550 MPN/100ml recorded at the EB site.

Table 8. Mean, median, and maximum Enterococcus levels (MPN/100ml) recorded at the EB and CB site TBWP stations between July 2020 and December 2021

Unit: MPN/100ml	Average	Median	Max.	% Exceedance
EB	209	29	15,550	25
CB	53	34	538	32

The time series of rainfall and Enterococcus concentration was further assessed to estimate the strength of the cross-correlation signal as a function of time lag between rain event occurrence and bacteria counts. The resulting plots shown in Figure 15 allow for inference of the time span taken by the rainfall runoff to elevate bacteria levels downstream in nearshore beach waters. Note that the cross-correlations between rainfall and bacteria level records fluctuated at the signal level below 1,000 several days after the associated rain event at both sites. Therefore, the correlation signal = 1,000 was considered as a common threshold value and the last day before the correlation level fell below this threshold was counted as a longest lag.

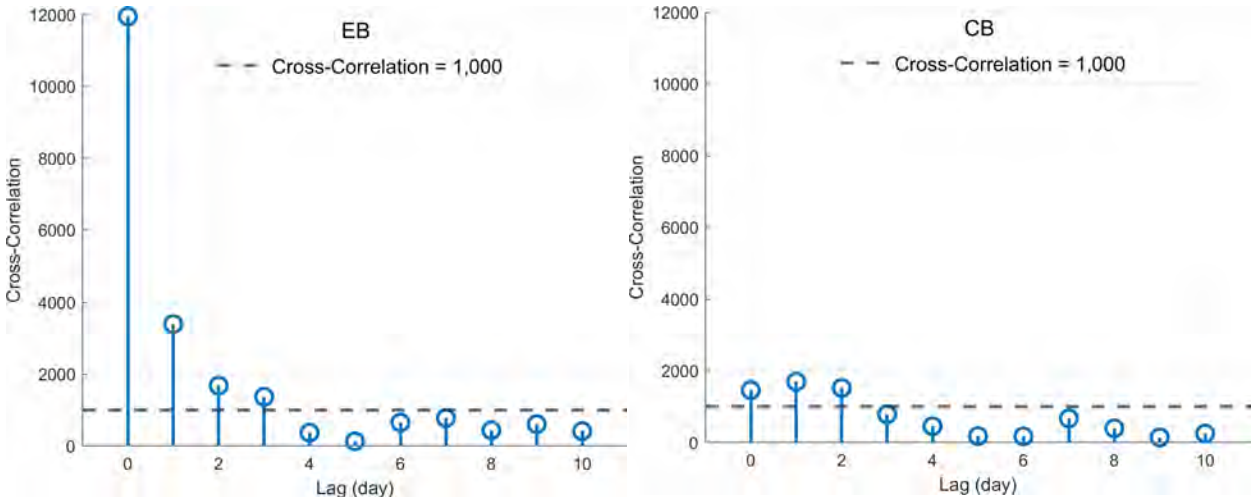

Figure 15. Cross-correlation between time series of the rainfall record and Enterococcus bacteria levels as a function of the lag in time of occurrence. The 24-hour total precipitation and daily maximum bacteria level recorded at the EB (left) and CB (right) sites are the two input variables used in this cross-correlation analysis.

The change in the correlation signals shows that at both sites bacteria levels in beach waters tend to respond to precipitation events instantaneously on the day of the rainfall event (lag = 0). At the EB site (left plot in Figure 15) the correlation rapidly reduces within the first day after a rain event but the signal level remained significant (> 1,000) for the additional three days. For the CB site (right plot in Figure 15) bacteria levels remain elevated (> 1,000) for up to the next two days after a rain event. The correlation was much pronounced at the EB site during the first two days after a rain. This may be an effect of large contributing area formed in the EB site that drains to the beach catchment.

Additionally, the linear dependence between measured rainfall and bacterial levels was quantified based on Pearson's parametric test. The slope of the least-squares reference line (solid) drawn in the comparison between daily precipitation record and daily maximum Enterococcus concentration shown in Figure 16 is equal to the correlation coefficient, *r,* indicating the strength and direction of the linear relationship between the two parameters. The values of r = -1 and 1 means a perfect negative and positive correlation, respectively, and r = 0 indicates no linear relationship between the two variables. For both the EB and the CB site, a positive correlation was estimated with respective values of r = 0.81 and r = 0.89. The minimum value of the Enterococcus bacterial level considered for this Pearson's test was 35 MPN/100ml.

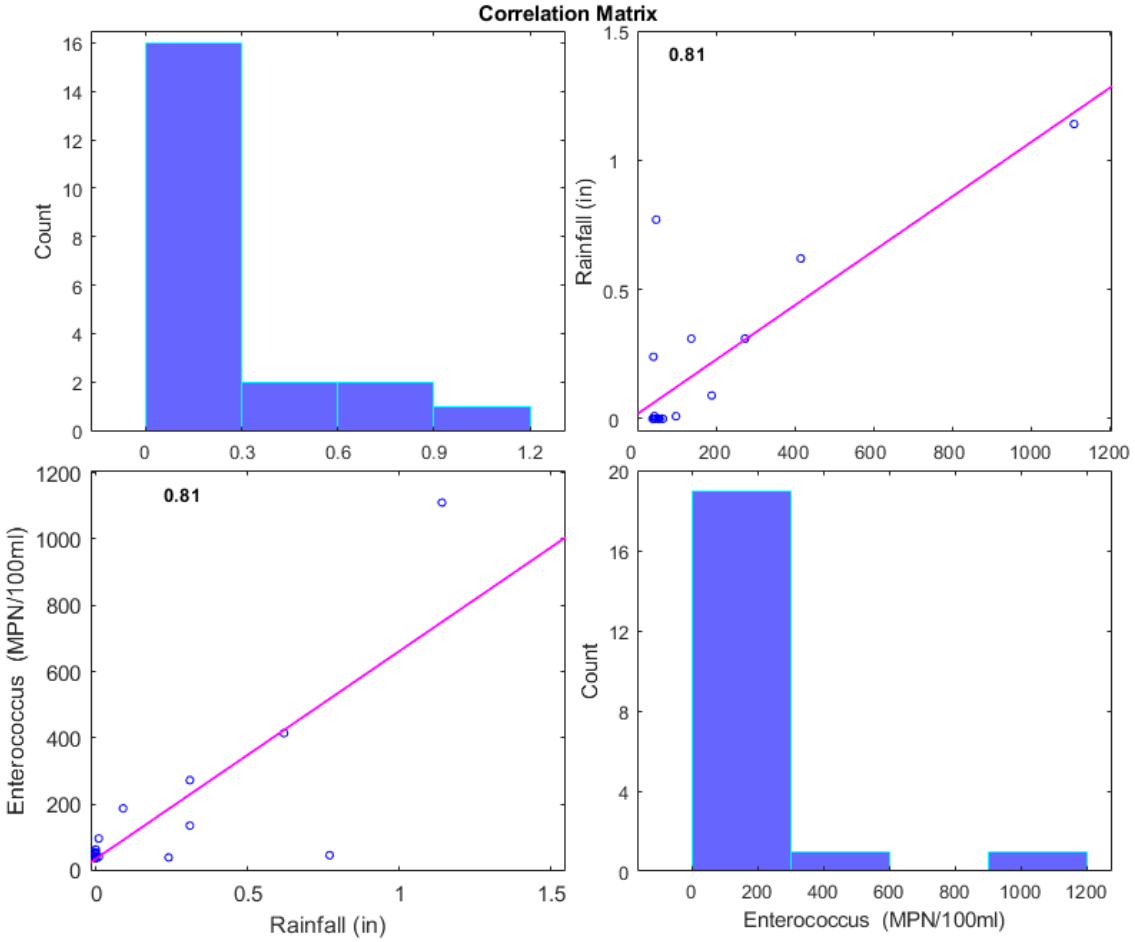

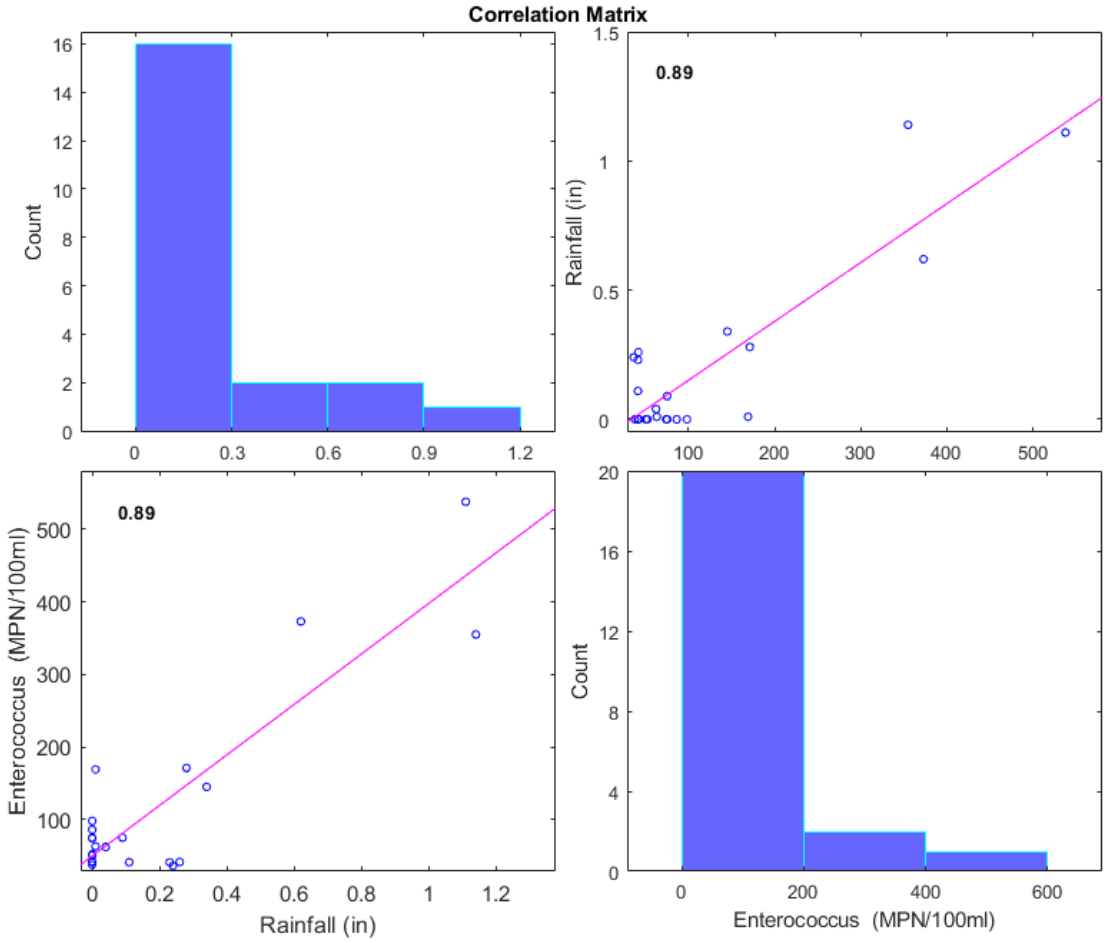

Figure 16. Histogram and correlation coefficients computed for the time series of two variables: rainfall record and Enterococcus bacteria levels for the EB site (top panels) and the CB site (bottom panels). The numbers shown in the scatter plots are the respective slopes of the least-squares reference lines, *r,* between the variable pair. The statistical analysis of the daily record of rainfall and maximum Enterococcus concentration indicates that there is a linear dependency between the two parameters. For both sites, the coastal waters at the runoff discharge location tended to respond to rainfall by elevating bacterial levels immediately following the rain event. Bacteria levels remained elevated for up to three days past a rain event at the CB site.

5 Summary and Discussion

The present study investigated rainwater runoff impacts on urbanized beaches situated at an eastern and a central location on Galveston Island. Runoff catchment characteristics were assessed by analyzing refined regional DEMs combined with national land use and hydrologic soil database information. Potential runoff stream patterns and peak discharge rates Q_p estimated using a desktop hydrologic assessment were in line with the island's beach runoff issues identified during field

reconnaissance. The potential stream power of major runoff discharge flows was calculated for each beach site as the product of peak discharge rate and mean slope assessed from the runoff catchment analysis.

Beach surface erosion caused by runoff discharge to the target beach sites were measured by low-altitude photographic field topographic surveys after select rain events. The measured geomorphic properties of the eroded beach surface were compared to the potential power of the runoff stream to estimate the site-specific geomorphic law describing the runoff beach erosion as a function of runoff discharge rate and surface gradient over the major beach runoff catchment. The runoff sediment displacement relationship indicated that the erosion on the eastern beach is related to the runoff stream power with input peak discharge rate calculated based on hourly maximum rainfall depth. At the central site, the beach erosion was described effectively by the runoff stream power defined based on daily cumulative rainfall depth.

The statistical relationship between rainfall event and change in bacteria levels in nearshore coastal waters was investigated based on the record of Enterococcus concentration obtained from TBWP stations near the respective major beach runoff outlet. A linear dependency was found for both the eastern and the central beach site. Overall, the bacteria level increased immediately on the day of the rainfall but then reduced starting from the next day already at the eastern beach site. Elevated bacteria levels persisted for up to three days after the rain event at the central beach site.

The present study provides a framework for coastal stormwater research that is broadly applicable for assessing urban runoff impacts on downstream beach flooding, erosion, and water contamination. The geomorphic sediment transport law proposed in this report can serve as an effective coastal engineering and management tool to quantify beach sediment erosion caused by nuisance and extreme rain-induced flood events. Further improvements and verification of the proposed transport law, however, are encouraged through continued efforts of field data collection. Future research can make use of longer-term precipitation and water quality monitoring records to analyze the bacterial indicator trends based on geospatial relationships with coastal rainfall runoff events of various severities. This will help improve understanding of major pathways for non-point source (NPS) pollution inflow to coastal waters and support NPS pollutant mitigation plans and control practices.

6 Acknowledgements

This report was funded by Texas Coastal Management Program grant No. 21-060-005-C665 approved by the Texas Land Commissioner, providing financial assistance under the Coastal Zone Management Act of 1972, as amended, awarded by the National Oceanic and Atmospheric Administration (NOAA), Office for Coastal Management, pursuant to NOAA Award No. NA20NOS4190184. Additional support was provided by the Park Board of Trustees of the City of Galveston and Texas A&M University. The views expressed herein are those of the authors and do not necessarily reflect the views of NOAA, the U.S. Department of Commerce, or any of their subagencies.

7 References

Asquith, W.H., Roussel, M.C., 2004. Atlas of Depth-Duration Frequency of Precipitation Annual Maxima for Texas (Report No. 2004–5041), Scientific Investigations Report. U.S. Geological Survey, Austin, Texas. https://doi.org/10.3133/sir20045041

Bagnold, R.A., 1966. An Approach to the Sediment Transport Problem from General Physics. US Government Printing Office.

Bizzi, S., Lerner, D.N., 2015. The Use of Stream Power as an Indicator of Channel Sensitivity to Erosion and Deposition Processes. River Res. Appl. 31, 16–27. https://doi.org/10.1002/rra.2717

City of Galveston, 2003. City of Galveston Master Drainage Plan. City of Galveston.

Cleveland, T.G., Herrmann, G.R., Tay, C.C., Neale, C.M., Schwarz, M.R., Asquith, W.H., 2015. 0-6824. New Rainfall Coefficients – Including Tools for Estimation of Intensity and Hyetographs in Texas (Research Report No. FHWA/TX-15/0-6824-1). Texas Tech University, Lubbock, TX.

Dietrich, W.E., Bellugi, D.G., Sklar, L.S., Stock, J.D., Heimsath, A.M., Roering, J.J., 2013. Geomorphic Transport Laws for Predicting Landscape form and Dynamics, in: Wilcock, P.R., Iverson, R.M. (Eds.), Geophysical Monograph Series. American Geophysical Union, Washington, D. C, pp. 103–132. https://doi.org/10.1029/135GM09

Dietrich, W.E., Bellugi, D.G., Sklar, L.S., Stock, J.D., Heimsath, A.M., Roering, J.J., 2003. Geomorphic Transport Laws for Predicting Landscape Form and Dynamics. Predict. Geomorphol., Geophysical Monograph Series 103–132. https://doi.org/10.1029/135GM09

Ervin G. Otvos, 1999. Rain-Induced Beach Processes; Landforms of Ground Water Sapping and Surface Runoff. J. Coast. Res. 15, 1040–1054.

Galloway, D.L., Coplin, L.S., Ingebritsen, S.E., 2003. Effects of Land Subsidence in the Greater Houston Area, in: Agthe, D.E., Billings, R.B., Buras, N. (Eds.), Managing Urban Water Supply. Springer Netherlands, Dordrecht, pp. 187–203. https://doi.org/10.1007/978-94-017-0237-9_12

Gartner, J.G., 2016. Stream Power: Origins, Geomorphic Applications, and GIS Procedures. [WWW Document]. URL https://extension.umass.edu/riversmart/

Horton, R.E., 1945. Erosional Development of Streams and their Drainage Basins; Hydrophysical Approach to Quantitative Morphology. GSA Bull. 56, 275–370. https://doi.org/10.1130/0016-7606(1945)56[275:EDOSAT]2.0.CO;2

Howard, A.D., Kerby, G., 1983. Channel Changes in badlands. GSA Bull. 94, 739–752. https://doi.org/10.1130/0016-7606(1983)94<739:CCIB>2.0.CO;2

Kirkby, M., 1971. Hillslope Process-response Models Based on the Continuity Equation. Geology.

Li, M.-H., Chibber, P., 2008. Overland Flow Time of Concentration on Very Flat Terrains. Transp. Res. Rec. 2060, 133–140. https://doi.org/10.3141/2060-15

Meyer-Peter, E., Müller, R., 1948. Formulas for Bed-load transport. [publisher not identified], [Stockholm].

Morton, F.I., 1983. Operational Estimates of Areal Evapotranspiration and their Significance to the Science and Practice of Hydrology. J. Hydrol. 66, 1–76. https://doi.org/10.1016/0022-1694(83)90177-4

MRLC Consortium, 2011. National Land Cover Database 2011 (NLCD 2011).

Nachtergaele, J., Poesen, J., Govers, G., 2002. Ephemeral Gullies. A spatial and Temporal Analysis of their Characteristics, Importance and Prediction. Belgeo 2, 159–182.

National Research Council, 2008. Urban Stormwater Management in the United States. National Research Council, Washington, DC.

O'Neill, C.R., Jr., 1985. A Guide to Coastal Erosion Processes, in: Information Bulletin 199. Cornell Cooperative Extension, pp. 1–15.

Phillips, J.D., Slattery, M.C., 2007. Downstream Trends in Discharge, Slope, and Stream Power in a Lower Coastal Plain River. J. Hydrol. 334, 290–303. https://doi.org/10.1016/j.jhydrol.2006.10.018

Roussel, M.C., Thompson, D.B., Fang, X., Cleveland, T.G., Garcia, C.A., 2005. Time-Parameter Estimation for Applicable Texas Watersheds (Research Report No. HWA/TX-05/0–4696–2). U.S. Geological Survey, Texas Tech University, Lamar University, University of Houston.

Steegen, A., Govers, G., Nachtergaele, J., Takken, I., Beuselinck, L., Poesen, J., 2000. Sediment Export by Water from an Agricultural Catchment in the Loam Belt of Central Belgium. Geomorphology 33, 25–36. https://doi.org/10.1016/S0169-555X(99)00108-7

Texas General Land Office, 2015. Texas Beach Watch Program: Quality Assurance Project Plan. [WWW Document]. URL https://cgis.glo.texas.gov/Beachwatch/

TxDOT, 2016. Hydraulic Design Manual. Texas Department of Transportation. http://onlinemanuals.txdot.gov/txdotmanuals/hyd/index.htm

USDA, 2014. Soil Survey Geographic (SSURGO) database for Galveston County, Texas.

USDA-NRCS, 2010. Chapter 15 - Time of Concentration, in: Part 630 Hydrology National Engineering Handbook. Natural Resources Conservation Service, United States Department of Agriculture, Washington, DC.

USDA-SCS, 1947. Handbook of Channel Design for Soil and Water Conservation (No. SCS-TP-61). Soil Conservation Service, Washington, DC.

USEPA, 2012. Recreational Water Quality Criteria. Office of Water, United States Environmental Protection Agency 820-F-12–058.

USGS, 2017. 1/9th Arc-second Digital Elevation Models (DEMs) - USGS National Map 3DEP Downloadable Data Collection.

WEF and ASCE, 1992. Design and Construction of Urban Stormwater Management Systems (Manuals and Reports of Engineering Practice), MOP 77/WEF MOP FD-20. Water Environment Federation, New York, NY. https://doi.org/10.1061/9780872628557

8 Appendix

This section provides additional research products listed as individual task deliverables in the Project Work Plan (WorkPlanBudget 21-060-005-C665.docx).

8.1 A1 - Grain size and permeability data (T1-3)

Sediment samples of the surface soil were collected from each beach site during field reconnaissance conducted in March 2021. The cumulative distribution functions of beach sediment grain sizes determined by sieve analysis of each collected sediment sample are shown in Figure A-1 and the associated sediment size distribution statistical parameters are provided in Table A-1.

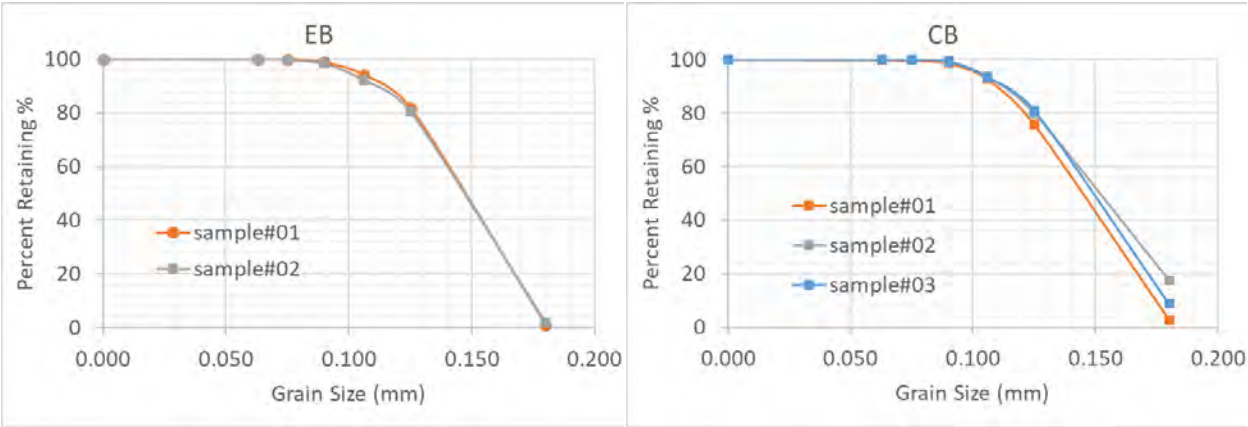

Figure A-1. Cumulative distribution functions for sediment grain size determined from beach surface grab samples collected in March 2021 at the two Galveston Island runoff study sites. Figure 5 and Figure 6 provide the sampling locations for the EB (left) and CB (right) sites, respectively.

Table A-1. Sediment size distribution statistical parameters for the EB and CB study sites

	EB	CB
Mean (mm)	0.15	0.16
Median (mm)	0.14	0.15
Std. Dev σ (mm)	0.14	0.14
Skewness SK_i	0.06	0.05
Kurtosis KG_i	0.92	0.83